

## Original Article

# The effect of basal topography on ice sheet dynamics

C. Schoof

Department of Earth and Ocean Sciences, University of British Columbia, 6339 Stores Road, Vancouver, V6T 1Z4, Canada  
(e-mail: cschoof@eos.ubc.ca)

Received August 20, 2002 / Accepted February 3, 2003  
Published online May 9, 2003 – © Springer-Verlag 2003  
Communicated by L. W. Morland

**Abstract.** Classical shallow-ice theory assumes that bed topography under ice sheets has slopes comparable to the surface slope of the ice sheet. A modification of the classical steady-state theory which allows for significant bed topography on shorter length scales has recently been developed by Morland (*Proc. R. Soc. L. Ser. A.*, 456, 1711–1739), but his theory requires explicit integration of the ice-flow equations over the topography length scale, which may be below the grid size of typical numerical ice sheet models. Here we present a method for parameterising the effect of basal topography of wavelengths much greater than ice thickness but much smaller than the horizontal extent of the ice sheet on the bulk flow of the ice sheet. In particular, we are able to show through the use of a multiple-scales expansion technique that the effect of such topography is described by a simple correction factor applied to the classical expression for ice flux. This correction factor dispenses with the need to integrate explicitly over the topography length scale and could allow the effect of such topography to be included in numerical models with limited grid size. Examples are given for the practical implementation of this ‘correction factor method’ in calculations of the steady-state shape of ice sheets.

**Key words:** ice sheets, shallow ice theory, lubrication flow, bed topography, multiple scales, homogenisation

## 1 Introduction

Classical lubrication or ‘shallow-ice’ theories for ice sheet flow [9] require that significant changes in basal topography occur only over length scales comparable with the horizontal extent of the ice sheet. In practice, ice sheets do have significant basal topography on shorter wavelength scales (see e.g. the BEDMAP project, <http://www.antarctica.ac.uk/aedc/bedmap/bedmap.html>, or [12], Fig. 6). Morland [7, 8] has addressed the question of how shallow ice models can be adapted to this case. His method, however, requires explicit integration over the length scale of basal topography. This renders his approach less useful for incorporation into numerical models, where basal topography on length scales at or below the grid spacing cannot be resolved.

Here we present an alternative approach to incorporating the effect of basal topography into dynamic shallow-ice models. The method used is based on the theory of homogenisation [6] and bears strong similarity with the treatment of classical sliding over ‘large’ bumps in [11]. It allows the ice flow problem over local topography to be parameterised in a large-scale ice sheet model, in much the same way as the problem of water flow in the pore space of a soil can be parameterised to give Darcy’s law for groundwater flow. This approach dispenses with the need to integrate explicitly over the topography length scale.

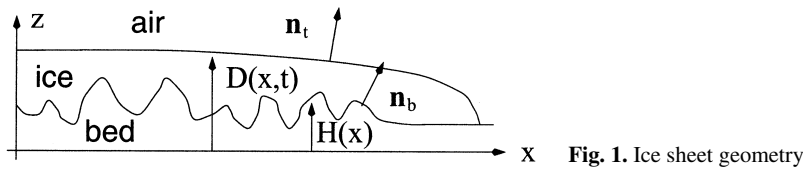


Fig. 1. Ice sheet geometry

We restrict ourselves to the case of topography length scales which are much greater than ice thickness and much shorter than the horizontal extent of the ice sheet; this is essentially the case which is treated in detail in Morland's papers [7,8]. Moreover, as in [7], we deal with an isothermal ice sheet.

## 2 Model

We consider a two-dimensional model for the incompressible slow viscous flow of ice over a given bed in two dimensions (Fig. 1). Given density  $\rho$ , acceleration due to gravity  $g$ , the velocity field  $\mathbf{u} = (u_1, u_2) = (u, w)$  and stress tensor  $\boldsymbol{\sigma}$  satisfy the usual field equations in Cartesian coordinates  $(x_1, x_2) = (x, z)$

$$\nabla \cdot \boldsymbol{\sigma} - \rho g \mathbf{k} = \mathbf{0}, \quad (1)$$

$$\nabla \cdot \mathbf{u} = 0, \quad (2)$$

where  $\mathbf{k}$  is the  $z$ -unit vector. Glen's law [10] gives the stress tensor as

$$\dot{\epsilon}_{ij} = \frac{1}{2} \left( \frac{\partial u_i}{\partial x_j} + \frac{\partial u_j}{\partial x_i} \right) = A \tau^{n-1} \tau_{ij}, \quad \tau = (\tau_{ij} \tau_{ji} / 2)^{1/2}, \quad (3)$$

where  $A$  is a constant (since we are assuming isothermal ice), and  $\boldsymbol{\tau}$  the deviatoric stress tensor, defined such that

$$\sigma_{ij} = \tau_{ij} - p \delta_{ij}. \quad (4)$$

Here,  $p$  denotes pressure,  $\delta_{ij}$  is the Kronecker delta and the summation convention is applied.

At the surface  $z = D(x, t)$  shear and normal stress vanish, hence

$$\mathbf{n}_t \cdot \boldsymbol{\sigma} = \mathbf{0}, \quad (5)$$

where  $\mathbf{n}_t$  is the unit normal to the surface.  $D(x, t)$  satisfies

$$\frac{\partial D}{\partial t} + u \frac{\partial D}{\partial x} = w + a \quad \text{on } z = D, \quad (6)$$

where  $a(x, t)$  denotes accumulation rate.

At the base  $z = H(x)$ , we define the basal shear stress vector

$$\boldsymbol{\tau}_b = \mathbf{n}_b \cdot \boldsymbol{\sigma} - (\mathbf{n}_b \cdot \boldsymbol{\sigma} \mathbf{n}_b) \mathbf{n}_b \quad \text{on } z = H, \quad (7)$$

where  $\mathbf{n}_b$  is the unit normal to the base. Basal velocity is assumed to satisfy a sliding law of the form derived in [1]:

$$\mathbf{u} = C |\boldsymbol{\tau}_b|^{n-1} \boldsymbol{\tau}_b \quad \text{on } z = H, \quad (8)$$

where  $C$  is a constant and  $n$  is the Glen's law exponent. The basal velocity thus defined is clearly parallel to the bed (since  $\mathbf{u} \cdot \mathbf{n}_b = 0$  on  $z = H$ ) and orientated in the direction of basal shear stress. Cavitation is neglected in the sliding law in (8) as the sliding velocity is independent of normal stress at the bed; unless drainage pressures are high, this is generally a good assumption for an ice sheet [2,3].

Depth-integration of (2) together with boundary conditions (6) and (8) gives the alternative form of mass conservation

$$\frac{\partial D}{\partial t} + \frac{\partial Q}{\partial x} = a : \quad Q(x, t) = \int_{H(x)}^{D(x,t)} u \, dz. \quad (9)$$

### 3 Non-dimensionalisation

We define the following scales:  $[u]$  for (horizontal) velocity,  $[\tau]$  for deviatoric stresses,  $[a]$  for accumulation rate,  $[D]$  for ice thickness and  $[L]$  for the lateral extent of the ice sheet (Fig. 2). As in standard shallow ice theory, we require the following balances for stress and velocity scales

$$[u]/[D] = [a]/[L] = 2A[\tau]^n, \quad [\tau] = \rho g[D]^2/[L], \quad (10)$$

which defines scales  $[u]$  for velocity,  $[\tau]$  for shear stress and  $[D]$  for thickness in terms of lateral extent  $[L]$  and accumulation rate  $[a]$ , which we take to be given.

Moreover, we suppose that there exists significant bed topography – of amplitude comparable to ice thickness  $[D]$ , though never penetrating through to the surface – which varies on a length scale  $[S]$ , where (cf. Fig. 2)

$$[D] \ll [S] \ll [L].$$

This allows two small parameters to be defined

$$\nu \doteq \frac{[D]}{[S]} \ll 1, \quad \delta \doteq \frac{[S]}{[L]} \ll 1$$

such that the aspect ratio of the ice sheet is  $\epsilon \doteq [D]/[L] = \nu\delta \ll 1$ .

As the bed topography varies on length scale  $[S]$  but the ice sheet has horizontal extent  $[L]$ , we define *multiply scaled* horizontal coordinates as

$$x = [S]x^* = [L]X^*, \quad (11)$$

and associated time variables as

$$t = [S]t^*/[u] = [L]T^*/[u]. \quad (12)$$

$(x^*, t^*)$  and  $(X^*, T^*)$  are of course not independent but related through  $(X^*, T^*) = \delta(x^*, t^*)$ . In the limit  $\delta \ll 1$  they may, however, be treated as independent in the context of a multiple scales expansion [6]. The ‘inner’ variables  $(x^*, t^*)$  describe local variations in ice flow while the ‘outer’ ones  $(X^*, T^*)$  are associated with the bulk flow of the ice sheet.  $x$ - and  $t$ -derivatives may then be expressed as

$$\frac{\partial}{\partial x} = \frac{1}{[S]} \left( \frac{\partial}{\partial x^*} + \delta \frac{\partial}{\partial X^*} \right), \quad (13)$$

$$\frac{\partial}{\partial t} = \frac{[u]}{[S]} \left( \frac{\partial}{\partial t^*} + \delta \frac{\partial}{\partial T^*} \right). \quad (14)$$

By analogy with [1, 11], we define a regional smoothed bed and surface (as might be used in a numerical model) by the running averages

$$[H]H^*(X^*) = \frac{1}{2L_M} \int_{-L_M}^{L_M} H(x + \xi) d\xi, \quad (15)$$

$$[H]D^*(X^*, t^*, T^*) = \frac{1}{2L_M} \int_{-L_M}^{L_M} D(x + \xi, t) d\xi, \quad (16)$$

where  $[S] \ll L_M \ll [L]$  so that the smoothed bed and surface only depend on the outer variable  $X^*$ . In practice, one might choose  $L_M = ([S][L])^{1/2}$ , so that  $[S]/[L_M] = [L_M]/[L] = \delta^{1/2} \ll 1$ . Note that the definitions in (15)–(16) only make sense at a distance from the ice sheet margin. Our theory thus does not allow for significant topography *at* the margin; this is indeed also true of Morland’s [7, 8] theory. Furthermore, the decomposition introduced above is only unique in the limit  $\delta \ll 1$ , provided that there is no significant bed topography at wavelengths intermediate between  $[S]$  and  $[L]$ .

If  $[d]$  denotes a scale for the local deviation of the ice surface elevation from its regional running average (Fig. 2), then the following dimensionless variables may be defined

$$z = [D]z^*, \quad (17)$$

$$D = [D]D^*(X^*, t^*, T^*) + [d]d^*(x^*, T^*, X^*, t^*), \quad (18)$$

$$H = [D]H^*(X^*, t^*, T^*) + [D]h^*(x^*, T^*, X^*, t^*), \quad (19)$$

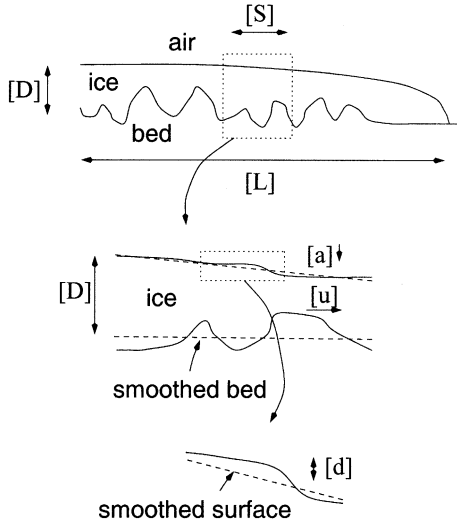


Fig. 2. Illustration of the scales used

$$\mathbf{u} = [u](u^*, \nu w^*), \quad \dot{\epsilon}_{ij} = [u]/(2[D])\dot{\epsilon}_{ij}^*, \quad \dot{\epsilon} = [u]/(2[D])\dot{\epsilon}^*, \quad (20)$$

$$Q = [u][D]Q^*, \quad a = [a]a^*, \quad (21)$$

$$\tau_{xz} = [\tau]\tau_{xz}^*, \quad \tau_{xx} = \nu[\tau]\tau_{xx}^*, \quad \tau_{zz} = \nu[\tau]\tau_{zz}^*, \quad (22)$$

$$p = \rho g([D]D^* + [d]d^* - [D]z^*) + \nu[\tau]p^*, \quad \tau_b = [\tau]\tau_b^*. \quad (23)$$

It remains to fix the scale  $[d]$  for local variations in ice surface elevation. Clearly one cannot have  $[d] = [D]$  since this would imply that the ice sheet has many ice divides; rather, one may expect that local  $O(1)$  variations in ice thickness due to basal topography (and hence potential  $O(1)$  variations in ice flux) lead to local  $O(1)$  variations in surface slope (which also lead to  $O(1)$  variations in ice flux). Thus we put

$$\frac{[d]}{[S]} = \frac{[D]}{[L]} \Rightarrow [d] = \delta[D]. \quad (24)$$

In fact, careful examination of Morland's [7] equations (4.4)<sub>1</sub> and (4.11) – bearing in mind the differences in notation – also suggests this scaling when the amplitude of bed undulations is  $O(1)$  compared with the ice thickness.

#### 4 Approximation scheme

The scaled variables defined by (11)–(22) are substituted in equations (1)–(9), and asterisks are omitted for convenience. All dependent variables are taken to be functions of the inner variables  $(x^*, t^*)$  as well as the outer ones,  $(X^*, T^*)$ , with the exception of the smoothed variables  $D^*$  and  $H^*$  as defined by (15) and (16). As is standard practice in multiple scales expansions, all dependent variables are required to be bounded functions of the inner variables  $x^*$  and  $t^*$ . (Specifically, all dependent variables must be bounded with respect to  $x^*$  varying over the entire real line, whereas boundedness with respect to inner time  $t^*$  can only be imposed for  $t^*$  greater than some finite value, say  $t^* > 0$ . The reason for this is that the time-reversed inner problem is one of backward diffusion, as will be seen in Sect. 4.3). Moreover, the definition of the smoothed variables  $D^*$  and  $H^*$  in (15)–(16) implies that (omitting asterisks)

$$\lim_{R \rightarrow \infty} \frac{1}{2R} \int_{-R}^R h(x, X) dx = 0, \quad (25)$$

$$\lim_{R \rightarrow \infty} \frac{1}{2R} \int_{-R}^R d(x, t, X, T) dx = 0. \quad (26)$$

The dimensionless model contains three parameters,  $\nu$ ,  $\delta$  and

$$\Gamma = C[\tau]^n/[u]. \quad (27)$$

We assume that sliding is not rapid, and thus put  $\Gamma = O(1)$ , while  $\nu, \delta \ll 1$ .

In view of  $\delta \ll 1$ , we reduce the domain  $H + h < z < D + \delta d$  to  $H + h < z < D$  and expand boundary conditions at the top surface in a Taylor series about  $z = D$ . To the error indicated, we obtain the following field equations on  $H + h < z < D$ ,

$$\frac{\partial}{\partial z} \left( \left| \frac{\partial u}{\partial z} \right|^{1/n-1} \frac{\partial u}{\partial z} \right) - \frac{\partial D}{\partial X} - \frac{\partial d}{\partial x} = O(\nu^2), \quad (28)$$

$$-2 \frac{\partial}{\partial z} \left( \left| \frac{\partial u}{\partial z} \right|^{1/n-1} \frac{\partial u}{\partial x} \right) + \frac{\partial}{\partial x} \left( \left| \frac{\partial u}{\partial z} \right|^{1/n-1} \frac{\partial u}{\partial z} \right) - \frac{\partial p}{\partial z} = O(\nu^2), \quad (29)$$

$$\frac{\partial u}{\partial x} + \frac{\partial w}{\partial z} = O(\delta), \quad (30)$$

while boundary conditions at  $z = D$  are

$$\left| \frac{\partial u}{\partial z} \right|^{1/n-1} \frac{\partial u}{\partial z} = O(\nu^2, \delta), \quad (31)$$

$$2 \left| \frac{\partial u}{\partial z} \right|^{1/n-1} \frac{\partial u}{\partial x} + p + \left( \frac{\partial D}{\partial X} + \frac{\partial d}{\partial x} \right) \left| \frac{\partial u}{\partial z} \right|^{1/n-1} \frac{\partial u}{\partial z} = O(\nu^2, \delta). \quad (32)$$

At the base  $z = H + h$ , boundary conditions become

$$u = \Gamma \left| \frac{\partial u}{\partial z} \right|^{1/n-1} \frac{\partial u}{\partial z} + O(\nu^2, \delta), \quad (33)$$

$$w = u \frac{\partial h}{\partial x} + O(\nu^2, \delta). \quad (34)$$

Lastly, integrated mass conservation can now be expressed as

$$Q = \int_{H+h}^D u \, dz + O(\delta), \quad (35)$$

$$\frac{\partial D}{\partial t} + \frac{\partial Q}{\partial x} + \delta \left( \frac{\partial D}{\partial T} + \frac{\partial d}{\partial t} + \frac{\partial Q}{\partial X} - a \right) = O(\delta^2). \quad (36)$$

The field equation (29) together with boundary condition (32) serves to determine the pressure field correction  $p$  once a solution for the velocity field  $u$  has been determined. As in ordinary shallow ice theory, both of these equations therefore decouple from the determination of the leading order solution (see also [5]).

#### 4.1 The outer problem

One of the main advantages of a multiple scales method is that one can often derive relations which involve only the outer coordinates,  $X$  and  $T$  in this case. The derivation of such an ‘outer’ problem avoids explicit integration over the inner coordinates and can be of great advantage if the main interest lies in determining quantities that depend only on the outer coordinates. In the present case, we are mostly concerned with determining the shape of the ice sheet  $D$ . As will be shown below,  $D$  turns out to be a function of  $X$  and  $T$  only at leading order, and its evolution can indeed be described by an equation involving only the outer coordinates  $X$  and  $T$ .

The tool we use for deriving a simplified equation for  $D$  is known as *homogenisation* (Holmes [6], Chap. 5), which involves averaging over the inner length and time scales. We define a spatial averaging operator  $\langle \cdot \rangle$  by analogy with [11]:

$$\langle f(x, t, X, T) \rangle = \lim_{R \rightarrow \infty} \frac{1}{2R} \int_{-R}^R f(x, t, X, T) \, dx, \quad (37)$$

where  $f$  can be any function for which this procedure is well-defined. One may note that  $\langle D \rangle = D$  and  $\langle H \rangle = H$  since  $D$  and  $H$  are independent of  $x$ , while  $\langle d \rangle = \langle h \rangle = 0$  by (25)–(26). Moreover, for any function  $f$  which is absolutely continuous and bounded with respect to the inner variable  $x$ , we have

$$\left\langle \frac{\partial f}{\partial x} \right\rangle = \lim_{R \rightarrow \infty} \frac{f(x = R) - f(x = -R)}{2R} = 0, \quad (38)$$

since  $f$  is bounded as a function of  $x$ .

The averaging operator in (37) differs from averaging operators typically encountered in homogenisation [6] by letting the limits of integration tend to infinity,  $R \rightarrow \infty$ , whereas homogenisation methods more commonly require the inner structure of the problem to be periodic. In the present problem, this would correspond to  $h$  and  $d$  periodic in the inner spatial coordinate  $x$  with some period  $\lambda$ , and  $\langle f \rangle$  for  $f$  periodic would be defined as

$$\langle f(x, t, X, T) \rangle = \frac{1}{\lambda} \int_0^\lambda f(x, t, X, T) dx. \quad (39)$$

However, if  $f$  is indeed periodic, then the two definitions of  $\langle f \rangle$  given above are equivalent. The reason for persisting with the definition in (37) is that, typically, short-wavelength variations in bed elevation  $h$  will not be periodic in  $x$ . The limit in (37) serves to remind one that a practical averaging length must lie ‘asymptotically’ between the length scales of interest, here the bed wavelength  $[S]$  and the ice sheet span  $[L]$ . We should point out that the averaging operator is never used if the limit in  $R$  is not assured to exist either by assumption through (25)–(26) or as a result of (38).

Applying  $\langle \cdot \rangle$  to both sides of (36) obtains, by (38),

$$\frac{\partial D}{\partial t} + \delta \left( \frac{\partial D}{\partial T} + \frac{\partial \langle Q \rangle}{\partial X} - \langle a \rangle \right) = O(\delta^2). \quad (40)$$

Hence

$$\frac{\partial D}{\partial t} = O(\delta) \quad (41)$$

and, as promised,  $D = D(X, T)$  depends only on the outer variables to  $O(\delta)$ . Specifically, changes in bulk ice sheet thickness occur on the time scale associated with the lateral extent of the ice sheet. Substituting in (36) then obtains

$$\frac{\partial Q}{\partial x} = O(\delta) \quad (42)$$

and  $Q = Q(X, t, T) + O(\delta)$ . Hence, in (40),  $\langle Q \rangle$  may be replaced by  $Q$  without changing the order  $O(\delta^2)$  of the error incurred.

We expand  $D$ ,  $d$ ,  $Q$  and  $u$  in the form

$$\begin{aligned} D &\sim D_0(X, T) + O(\nu^2, \delta), & d &\sim d_0(x, t, X, T) + O(\nu^2, \delta), \\ Q &\sim Q_0(X, t, T) + O(\nu^2, \delta), & u &\sim u_0(x, z, t, X, T) + O(\nu^2, \delta). \end{aligned} \quad (43)$$

From equations (28), (31) and (33) the following velocity field  $u_0$  can be calculated by simple quadrature:

$$\begin{aligned} u_0 = - &\left[ \frac{(D_0 - H - h)^{n+1} - (D_0 - z)^{n+1}}{n+1} + \Gamma (D_0 - H - h)^n \right] \times \\ &\left| \frac{\partial D_0}{\partial X} + \frac{\partial d_0}{\partial x} \right|^{n-1} \left( \frac{\partial D_0}{\partial X} + \frac{\partial d_0}{\partial x} \right). \end{aligned} \quad (44)$$

Formula (35) then allows ice flux to be computed

$$Q_0(X, t, T) = - \left[ \frac{(D_0 - H - h)^{n+2}}{n+2} + \Gamma (D_0 - H - h)^{n+1} \right] \left| \frac{\partial D_0}{\partial X} + \frac{\partial d_0}{\partial x} \right|^{n-1} \left( \frac{\partial D_0}{\partial X} + \frac{\partial d_0}{\partial x} \right). \quad (45)$$

Rearranging gives

$$-\frac{\partial D_0}{\partial X} - \frac{\partial d_0}{\partial x} = \left[ \frac{(n+2)}{[(D_0 - H - h) + (n+2)\Gamma] (D_0 - H - h)^{n+1}} \right]^{1/n} |Q_0|^{-1+1/n} Q_0. \quad (46)$$

Note that we require basal topography not to penetrate to the surface, and so to leading order  $D_0 > H + h$ , and the right-hand side of (46) is nowhere divergent. By averaging both sides of (46) and using (38), a relation between mean surface slope  $\partial D_0 / \partial X$ , flux  $Q_0$  and a weighted mean over ice thickness is obtained,

$$-\frac{\partial D_0}{\partial X} = [(n+2)]^{1/n} |Q_0|^{-1+1/n} Q_0 \left\langle \left[ \frac{1}{[(D_0 - H - h) + (n+2)\Gamma] (D_0 - H - h)^{n+1}} \right]^{1/n} \right\rangle, \quad (47)$$

where  $Q_0$  may be taken outside  $\langle \cdot \rangle$  since it is independent of  $x$ . From (47), we finally arrive at an expression for ice flux in which the effect of local bed topography is parameterised in terms of a correction factor  $\theta$ ,

$$Q_0 = -\theta(D_0, X) \left[ \frac{(D_0 - H)^{n+2}}{n+2} + \Gamma(D_0 - H)^{n+1} \right] \left| \frac{\partial D_0}{\partial X} \right|^{n-1} \frac{\partial D_0}{\partial X}, \quad (48)$$

where

$$\theta(D_0, X) = \left\langle \left[ \frac{1}{\left[ 1 - \frac{h}{D_0 - H + (n+2)\Gamma} \right] \left( 1 - \frac{h}{D_0 - H} \right)^{n+1}} \right]^{1/n} \right\rangle^{-n}. \quad (49)$$

Since none of the quantities on the right-hand sides of (48) and (49) depend on the inner time coordinate  $t$ , we conclude that the ice flux  $Q_0$  is a function of  $X$  and  $T$  only,  $Q_0(X, T)$ .

By analogy with (37), a time-averaging operator may be defined as

$$\langle f(x, X, t, T) \rangle_t = \lim_{R \rightarrow \infty} \frac{1}{R} \int_0^R f(x, X, t, T) dt. \quad (50)$$

An analogue of (38) now states that

$$\left\langle \frac{\partial f}{\partial t} \right\rangle_t = \lim_{R \rightarrow \infty} \frac{f(t=R) - f(t=0)}{R} = 0, \quad (51)$$

which reveals the rationale for integrating only over  $(0, R)$ , as  $f$  may not be bounded for  $t \rightarrow -\infty$ . Applying  $\langle \cdot \rangle_t$  to (36) finally yields

$$\frac{\partial D_0}{\partial T} + \frac{\partial Q_0}{\partial X} = \langle \langle a \rangle \rangle_t, \quad (52)$$

which is the expected outer problem.

#### 4.2 The correction factor

If  $\theta$  in (48) is set to unity, the classical shallow-ice expression for ice flux is obtained.  $\theta$  thus describes the effect of local topography on ice flux. It is straightforward to see that  $\theta = 1$  when local bed topography vanishes ( $h \equiv 0$  at some given  $X$ ), and it is furthermore possible to show quite generally that  $\theta \leq 1$ , with equality holding if and only if  $h \equiv 0$  (see appendix A).

Note that we have written  $\theta$  as a function of  $D_0$  and  $X$ , as this is the form in which it is most likely to appear in applications. In ordinary shallow-ice theory ( $\theta \equiv 1$ ), (52) is a degenerate diffusion equation for  $D_0$  with diffusion coefficient  $(D_0 - H)^{n+2}/(n+2) + \Gamma(D_0 - H)^{n+1}$ . The nature of (52) does not change fundamentally if an additional positive factor  $\theta$ , depending only on  $D_0$  and position  $X$ , is introduced into this diffusion coefficient, provided  $\theta$  does not vanish anywhere. From a practical point of view, the main difficulty lies in calculating (or at least estimating) the diffusion coefficient at a given  $D_0$  and for a given bed with small-scale topography.

The most obvious method for incorporating the factor  $\theta$  into a practical ice sheet model (where we assume a fixed grid for simplicity) would be the following: Given data on the bed elevation near a fixed grid point  $X$ , calculate a smoothed bed  $H$  by averaging over some length scale  $L_M$  (which must be considerably greater than the grid spacing, but much smaller than the size of the ice sheet). Then calculate  $h$  near the grid point from the same data by subtracting the value of  $H$  calculated at the grid. Subsequently, using the values for  $H$  and  $h$  obtained, calculate  $\theta$  at grid point for some representative set of values of  $D_0$ , using (49) with the same finite averaging length scale  $L_M$  replacing the limit in  $R$  in the definition of  $\langle \cdot \rangle$  in (37). To find  $\theta$  for values of  $D_0$  not lying in that set, some interpolation scheme should then be used.  $\theta(D_0, X)$  is then represented at each grid point  $X$  by some locally defined interpolating function with argument  $D_0$ . Note that, because local bed topography must not penetrate to the surface,  $\theta$  is only defined for  $D_0 - H$  greater than the maximum of  $h$  at a given outer position  $X$ . In fact, as  $D_0 - H$  approaches that maximum,  $\theta$  tends to zero (cf. Fig. 3).

In the context of choosing an appropriate grid spacing, it is worth pointing out that the error incurred in our model is of  $O(\nu^2, \delta)$ . If the overall ice sheet aspect ratio  $\epsilon = \nu\delta$  – the small parameter which underlies the reductions in standard shallow ice theory – is fixed, then the error in our model is minimised if  $\delta \sim \nu^2$ , corresponding to  $\nu \sim \epsilon^{1/3}$ . For a typical ice sheet aspect ratio of  $10^{-3}$ , this occurs when  $\nu \sim 0.1$ . With a lateral

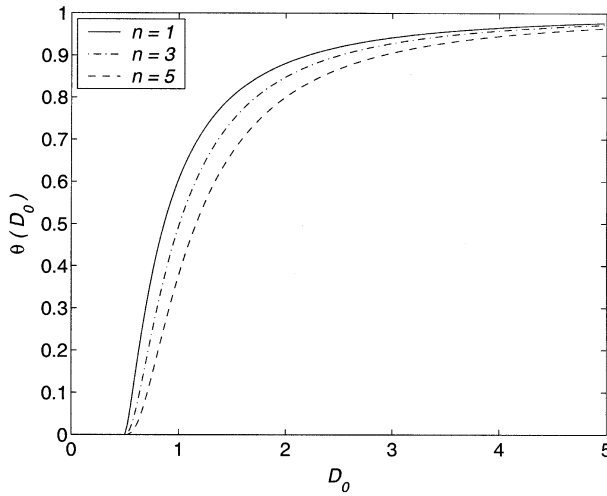


**Fig. 3.** The correction factor  $\theta(D_0)$  for a locally sinusoidal bed with amplitude 0.5,  $h = 0.5 \sin(x)$ , and with sliding parameter  $\Gamma = 1$ , at different values of the Glen exponent  $n$ .  $H$  is set to zero. Note that  $\theta$  tends to zero as  $D_0$  approaches the amplitude of  $h$ , and that  $\theta$  approaches unity when  $D_0$  is large

extent of 1000 km, this corresponds to a local topography length scale of 10 km. The outer model thus works best if it is used to parameterise local topography of length scales around 10 km. Bed topography on much larger length scales than 10 km should then be resolved explicitly through the smoothed bed height  $H$  rather than the correction factor  $\theta$ . Similarly, the correction factor method cannot be used at the margins as explained above, as the smoothing process cannot be applied. Consequently, local bed topography there has to be resolved explicitly in terms of the bed height  $H$ , which may require some grid refinement near the margin.

#### 4.3 The inner problem

Once the outer problem has been solved, it is straightforward to derive a more detailed solution for the flow field, valid on the inner length scale associated with coordinates  $x$  and  $t$ .

Relation (46) can be used to recover an expression for the local correction term  $d_0$  to ice surface elevation  $D_0$  once  $D_0$  and  $Q_0$  have been computed. Specifically,

$$\frac{\partial d_0}{\partial x} = -\frac{\partial D_0}{\partial X} - \left[ \frac{(n+2)Q_0}{[(D_0 - H - h) + (n+2)\Gamma] (D_0 - H - h)^{n+1}} \right]^{1/n}. \quad (53)$$

For local bed topography  $h$  which is periodic in the inner coordinate  $x$ , this allows  $d_0$  to be calculated given  $D_0$ ,  $H$  and  $h$  if we impose further that the mean of  $d_0$  must be zero.

Equation (53) essentially shows that  $\partial d_0 / \partial x$  adjusts such that ice flux varies only on the long length scale  $[L]$  but not over the topography length scale  $[S]$ . Clearly, this may conflict with initial conditions which one could impose on local ice surface topography; if initially  $\partial d_0 / \partial x$  does not take the required form (and hence  $\partial Q / \partial x = O(1)$  rather than  $O(\delta)$ ), one rescales time as  $t^{**} = t^* / \delta$ . The resulting, rescaled inner problem is one of non-linear (but non-degenerate) diffusion,

$$\frac{\partial d_0}{\partial t^{**}} - \frac{\partial}{\partial x} \left\{ \left[ \frac{(D_0 - H - h)^{n+2}}{n+2} + \Gamma (D_0 - H - h)^{n+1} \right] \left| \frac{\partial D_0}{\partial X} + \frac{\partial d_0}{\partial x} \right|^{n-1} \left( \frac{\partial D_0}{\partial X} + \frac{\partial d_0}{\partial x} \right) \right\} = 0, \quad (54)$$

where asterisks have been re-introduced on the time variable  $t^{**}$  for definiteness. Owing to the diffusive nature of this problem, one may expect  $d_0$  to relax rapidly – over times of  $O(\delta^2)$  compared with the outer time scale  $[T]$  – to the steady-state form given by (53). Thus, at times  $T$  strictly of  $O(1)$ , the results derived here are valid regardless of initial conditions.

Once  $\partial d_0 / \partial x$  is known, the velocity field  $u_0$  can be computed from (44); the corresponding vertical velocity component  $w_0$  can then finally be calculated from (30) and (34). This calculation is straightforward, though somewhat tedious, and we do not give details here.

## 5 A practical example

As an example of how the correction factor method can be put into practice, we consider the case of a steady ice sheet. This is also the case considered in Morland's work [7,8], which facilitates comparison. If we take flux  $Q$  to be given by (45) and require that  $D$ ,  $d$  and  $a$  are independent of time (subscripts  $_0$  will henceforth be omitted), then (36) essentially becomes Morland's [8] 'enhanced reduced' model equation (62) expanded in multiple scales, with some minor changes in the flux prescription – for instance, temperature is constant here and the sliding law employed by Morland is slightly different from ours. We have also set Morland's bed slope terms  $\chi_f$  and  $\Delta_f$  to unity, incurring an error of  $O(\nu^2)$  in our notation, which is the order to which the model is valid in any case.<sup>1</sup> Our leading-order model therefore has the same accuracy as Morland's [7,8] enhanced reduced model, and the subsequent higher-order corrections derived by Morland have no equivalent here. The method presented in Sect. 4.1 has shown how this enhanced reduced model can be simplified using multiple scales when  $\delta \ll 1$  to give an outer problem of the form (52) with  $a$  and  $D$  time-independent, and where  $Q$  is given in terms of 'outer' quantities by (48) and (49).

In order to establish how well this homogenisation method performs at describing the averaged effect of local bed topography, we solve explicitly the steady-state ice sheet problem

$$\begin{aligned} \frac{dQ}{dX} &= a(X), \\ Q(X) &= - \left[ \frac{(D(X) - H(X) - h(X/\delta, X))^{n+2}}{n+2} + \Gamma(D(X) - H(X) - h(X/\delta, X))^{n+1} \right] \times \\ &\quad \left| \frac{dD}{dX} \right|^{n-1} \frac{dD}{dX}, \end{aligned} \quad (55)$$

where  $\delta$  is small but finite, and  $a$ ,  $H$  and  $h$  are prescribed functions (we avoid any complications due to accumulation rate being elevation-dependent here for simplicity). Boundary conditions are that flux  $Q$  and ice thickness  $D - H - h$  vanish at the as yet undetermined margins. There are thus two more boundary conditions than the solution of a second-order ordinary differential boundary value problem requires, and these extra conditions serve to determine the position of the margins. This amounts to a solution of Morland's [7,8] enhanced reduced model with the slope factors  $\chi_f$  and  $\Delta_f$  set to unity and no temperature variations. This solution is then compared with a solution of the corresponding correction factor model

$$\begin{aligned} \frac{dQ}{dX} &= a(X), \\ Q(X) &= -\theta(D, X) \left[ \frac{(D(X) - H(X))^{n+2}}{n+2} + \Gamma(D(X) - H(X))^{n+1} \right] \left| \frac{dD}{dX} \right|^{n-1} \frac{dD}{dX}, \end{aligned} \quad (56)$$

where  $\theta(D, X)$  is defined in terms of the local bed topography  $h(x, X)$  through (49). In practice, we choose  $h$  to be periodic in its first argument with unit period, so the integral in (49) is taken simply over one period in the inner coordinate  $x$ :

$$\theta = \left\{ \int_0^1 \left[ \frac{1}{\left[ 1 - \frac{h(x, X)}{D(X) - H(X) + (n+2)\Gamma} \right] \left( 1 - \frac{h(x, X)}{D(X) - H(X)} \right)^{n+1}} \right]^{1/n} dx \right\}^{-n}. \quad (57)$$

Note that  $h = 0$  is required at the margin for the correction factor method, and so  $Q = 0$  and  $D - H = 0$  are the appropriate boundary conditions at the margins for the correction factor method.

The method used to calculate solutions is very similar to Morland's [7,8] shooting method. With a prescribed accumulation rate  $a(X)$ , it is possible to determine the margin positions explicitly once the ice divide location is known (cf. [4], p. 334). For a given guess of divide position, the left and right margin positions are therefore calculated explicitly, and (55) (or (56)) is integrated using a fourth-fifth order Runge-Kutta method from each margin to the divide. To avoid singularities at the margins, a change of variable  $S = (D - H)^{(2n+1)/n}$  is performed first. In the case of (56), the correction factor  $\theta$  is calculated explicitly at each integration step using

<sup>1</sup> Note that Morland's  $\delta$  corresponds to our  $\nu$ .

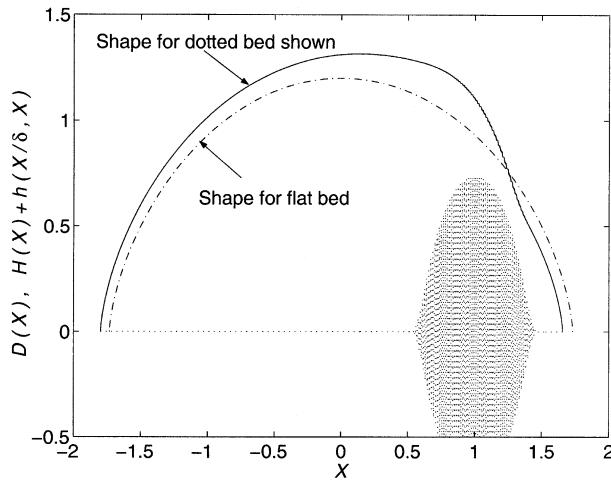


**Fig. 4.** Numerical calculation of the steady-state surface of an ice sheet with the parameter choices shown in Sect. 5. The bed shape is shown as a dotted line, while the solution of Morland's [7] enhanced reduced model and of the correction factor model are shown as solid and dashed lines, respectively. The two solutions are virtually indistinguishable. For comparative purposes, the steady-state solution for a completely flat bed ( $h = 0$ ) is also shown as a dot-dashed line

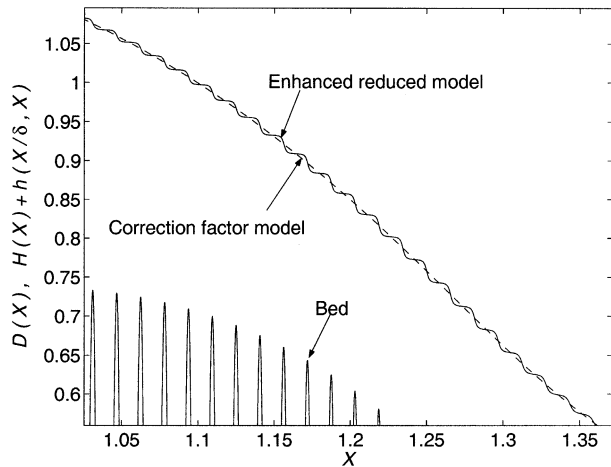


**Fig. 5.** An enlargement of the solutions of the enhanced reduced model (*solid line*) and the correction factor (*dashed line*) model shown in Fig. 4. The bed is now shown as a solid line (*bottom left*). Clearly, the enhanced reduced and correction factor models agree closely, but the correction factor model, being concerned with the outer length scale, does not reproduce the short length-scale wiggles in the ice sheet surface

32-point Gauss-Legendre quadrature, with an estimated fractional quadrature error of  $10^{-14}$ . The ice divide position is then found by requiring that the left and right solutions match at the divide, which is achieved by using Newton's method on the difference between left and right solutions for  $S$  at the trial position for the divide.

Figures 4 and 5 show results for the following choices:  $\delta = 1/64$ ,  $\Gamma = 1$ ,  $n = 1$ ,  $a(X) = 1 - X^2$ ,  $H \equiv 0$  and

$$h(x, X) = \begin{cases} 2 \exp\left(\frac{-0.25}{(X-0.5)(1.5-X)}\right) \cos(2\pi x) & 0.5 < X < 1.5, \\ 0 & \text{otherwise,} \end{cases} \quad (58)$$

which ensures that  $h$  is smooth and vanishes at the margins provided the right margin position is greater than 1.5. In Fig. 4, the two solutions are so close together as to be indistinguishable. The close-up in Fig. 5 is necessary to reveal the difference. In terms of computational expense, the correction factor method fared considerably better than direct integration: for a variety of error tolerances imposed on the Runge-Kutta solver, the computation time for the correction factor method was typically 5% of that required for direct integration, despite the fact that the correction factor was computed explicitly at each integration step.

Figure 4 also shows that bed topography on short length scales does alter the shape of the steady-state ice sheet significantly: the dot-dashed line shows the steady-state ice sheet surface for the same parameter choices but with a perfectly flat bed,  $h \equiv 0$ . Clearly, the presence of local bed topography has led to the mean ice sheet thickness becoming greater. Also, the ice sheet has become noticeably asymmetrical, with a bulge near the 'rough' bed patch.

Results for the bed defined by (58) and the same parameter values as above, but with the Glen's law exponent set to the more widely used value of  $n = 3$ , are plotted in Figs. 6 and 7. The same conclusions regarding the performance of the correction factor model apply. In Fig. 6 the plots of the enhanced reduced model and

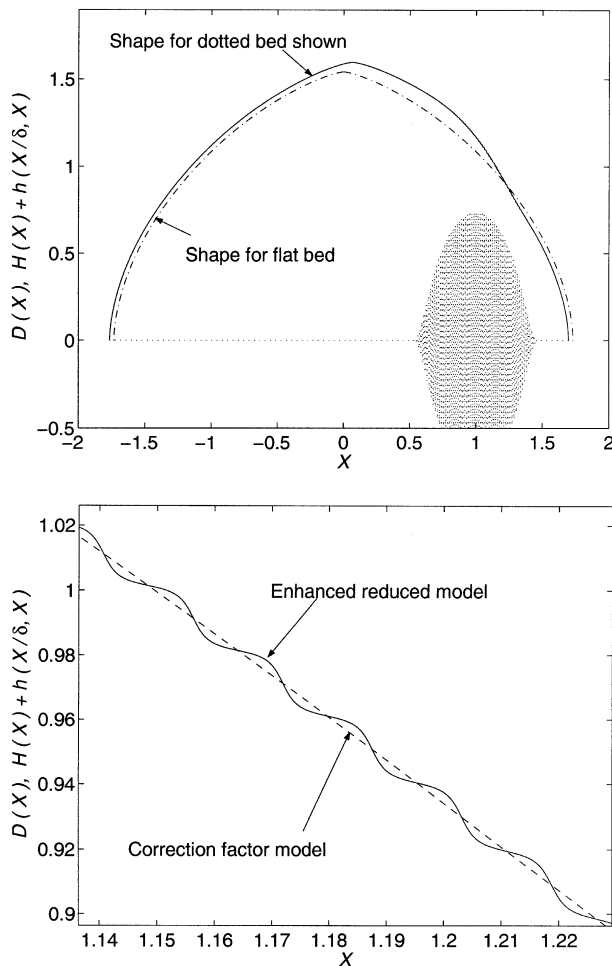


**Fig. 6.** Numerical calculation of the steady-state surface of an ice sheet with the same parameter choices as used for Figs. 4–5, except  $n = 3$ , which is more widely used to describe ice rheology. The bed shape is shown as a dotted line, while the solution of the enhanced reduced model and correction factor model are shown as solid and dashed lines, respectively. As before, the two solutions are virtually indistinguishable. As in Fig. 4, the steady-state solution for a completely flat bed ( $h = 0$ ) is also shown as a dot-dashed line

**Fig. 7.** An enlargement of the solutions of the enhanced reduced model (solid line) and the correction factor (dashed line) model shown in Fig. 6

correction factor model results are virtually indistinguishable, and a close-up is required to separate the short-wavelength wiggles of the enhanced reduced model solution from the smoothed solution of the correction factor method. The main difference here is that bed topography has a smaller effect on the steady-state configuration of the ice sheet than for  $n = 1$ . This may be attributed to the fact that mean ice thickness is greater for  $n = 3$  than  $n = 1$  (compare Figs. 4 and 6), so that the bed topography amplitude is smaller compared with the mean ice thickness, which is clearly likely to lessen its effect.

In Fig. 8 we present results for a case in which the correction factor method may be expected not to perform well. The same parameter values were used as for the calculations depicted in Figs. 4–5:  $\Gamma = 1$ ,  $n = 1$ ,  $a(X) = 1 - X^2$ , and  $H \equiv 0$ , but we set  $\delta = 1/5$ , so that bed topography has wavelengths not very dissimilar to the span of the ice sheet. The surface bumps caused by bed topography are now much more prominent in the enhanced reduced model solution, giving the ice sheet surface a number of prominent bulges which are, for obvious reasons, not reproduced by the correction factor method. However, what is remarkable here is the close agreement between the correction factor and enhanced reduced model solutions in regions where there is no bed topography ( $X < 0.5$  and  $X > 1.5$ ). In fact, the margin and ice divide positions calculated by the two methods agree to a fractional error of about  $10^{-3}$ , which is much smaller than the  $O(\delta^2) \approx 4 \times 10^{-2}$  error which is expected of the correction factor method.

## 6 Discussion

We have presented a formalism for incorporating the effect of ‘local’ bed topography into ice sheet models which deal solely with dynamics on the ice sheet length scale. Our method has shown that such topography can be

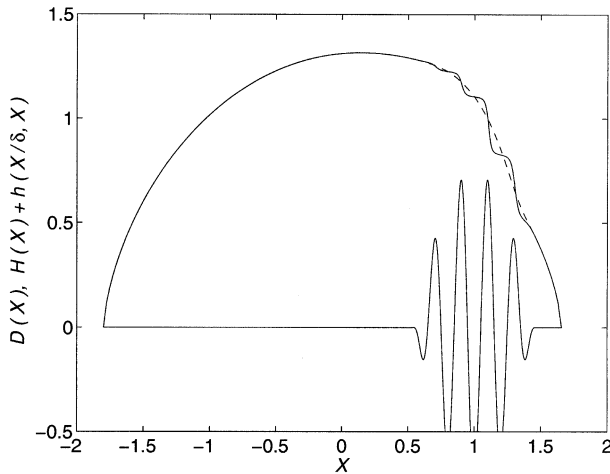


**Fig. 8.** Numerical calculation of the steady-state surface of an ice sheet with the same parameter choices as used for Figs. 4–5, except  $\delta = 1/5$ , so that the bed has a much longer wavelength. The bed shape is shown as a solid line, while the solution of the enhanced reduced model and correction factor model are shown as solid and dashed lines, respectively. The enhanced reduced model and correction factor model solutions now differ noticeably over the region with non-zero bed topography, where the correction factor method fails to reproduce the surface bulges calculated by the enhanced reduced model. The reason for this is obviously the smoothing involved in the correction factor method, which considers these bulges as small perturbations to the surface (In fact, the correction factor solution is unchanged from that shown in Fig. 4). Remarkably, however, the two solutions still agree closely where bed topography vanishes

described for an isothermal ice sheet through a correction factor  $\theta$  which reduces the ice flux computed from a regionally smoothed bed and surface. The results of Sect. 5 have shown that, for extended topography, the ice sheet model based on the correction factor approach yields results in close agreement with a model which integrates directly over the topography length scale. As Fig. 8 shows, this holds even when the bed wavelength and ice sheet span are not particularly well separated.

If local topography consists of isolated features, then (49) suggests that  $\theta \approx 1$ , so only extended topography is likely to have a significant effect, as already suggested by Morland [7]. In fact, for isolated local bed features, a boundary layer method may be more appropriate than the present approach using the method of homogenisation, which usually assumes that local ‘structure’, in this case bed topography, is quasi-periodic.

In this paper, sliding has been described by a sliding law of the form  $u_b = C\tau_b^n$ . The method used is, however, not dependent on this particular parameterisation of sliding. If a different sliding law is used, it is merely the inversion of (45) to give (46) that may not be possible analytically, and a closed form solution of the correction factor may thus not be available for other sliding laws (specifically ones which have  $u_b \not\propto \tau_b^n$ ).

Lastly, the extension of the present work to three dimensions is trivial. If  $\mathbf{X} = (X, Y)$  denotes horizontal position, one obtains the following model applicable at the long length scale  $[L]$ :

$$\frac{\partial D}{\partial T} + \nabla \cdot \mathbf{Q} = a, \quad (59)$$

$$\mathbf{Q} = -\theta(D, \mathbf{X}) \left( \frac{1}{n+2} (D-H)^{n+2} + \Gamma (D-H)^{n+1} \right) |\nabla D|^{n-1} \nabla D. \quad (60)$$

Here  $\nabla = (\partial/\partial X, \partial/\partial Y)$  and  $\theta$  is still given by (49), but  $\langle \cdot \rangle$  now has to be understood as a two-dimensional regional average. Crucially, we see that the effect of bed topography on this length scale is isotropic at leading order in a three-dimensional model.

*Acknowledgement.* This manuscript benefited greatly from the helpful comments of Leslie Morland and an anonymous reviewer. An earlier draft was improved by comments from Andrew Fowler. Financial support in the form of a Killam postdoctoral fellowship at the University of British Columbia is gratefully acknowledged.

## A Appendix

The function

$$f(y) = \frac{1}{(1-\alpha y)^{1/n} (1-\beta y)^{1+1/n}}$$

is convex for  $\alpha, \beta > 0$  and  $y < \min(\alpha^{-1}, \beta^{-1})$ , so

$$\frac{1}{x_2 - x_1} \int_{x_1}^{x_2} f(y(x)) dx \geq f\left(\frac{1}{x_2 - x_1} \int_{x_1}^{x_2} y(x) dx\right)$$

provided  $\max_{x \in [x_1, x_2]} y(x) < \min(\alpha^{-1}, \beta^{-1})$ . Hence, with  $y = h(x)$ ,  $\alpha = (D_0 - H + (n+2)\Gamma)$ ,  $\beta = (D_0 - H)$  and  $x_2 = -x_1 = R$ ,  $R \rightarrow \infty$ , we have

$$\lim_{R \rightarrow \infty} \frac{1}{2R} \int_{-R}^R y(x) dx = \langle h \rangle = 0, \quad (61)$$

and hence (since  $f(0) = 1$ )

$$\theta^{-1/n} = \lim_{R \rightarrow \infty} \frac{1}{2R} \int_{-R}^R f(y(x)) dx \geq 1. \quad (62)$$

Finally, this implies

$$\theta \leq 1, \quad (63)$$

where equality holds if and only if  $h \equiv 0$ . Thus the presence of basal topography on the length scales considered *impedes* ice flow, as may be expected intuitively.

## References

1. Fowler, A. C.: A theoretical treatment of the sliding of glaciers in the absence of cavitation. *Phil. Trans. R. Soc. L.* **298** (1445), 637–685 (1981)
2. Fowler, A. C.: A sliding law for glaciers of constant viscosity in the presence of subglacial cavitation. *Proc. R. Soc. L. Ser. A* **407**, 147–170 (1986)
3. Fowler, A. C.: Sliding with cavity formation. *J. Glaciol.* **33**(105), 255–267 (1987)
4. Fowler, A. C.: *Mathematical Models in the Applied Sciences*. Cambridge Texts in Applied Mathematics. Cambridge: Cambridge University Press (1997)
5. Fowler, A. C., Larson, D. A.: On the flow of polythermal glaciers. i. model and preliminary analysis. *Proc. R. Soc. L. Ser. A.* **363**, 217–242 (1978)
6. Holmes, M. H.: *Introduction to Perturbation Methods*, volume 20 of *Texts in Applied Mathematics*. New York: Springer (1995)
7. Morland, L. W.: Steady plane isothermal linearly viscous flow of ice sheets on beds with moderate slope topography. *Proc. R. Soc. L. Ser. A.* **456**, 1711–1739 (2000)
8. Morland, L. W.: Influence of bed topography on steady plane ice sheet flow. In Straughan, B., Greve, R., Ehrentraut, H., Wang, Y. (editors): *Continuum Mechanics and Applications in Geophysics and the Environment*, pages 276–304. Berlin: Springer (2001)
9. Morland, L. W., Johnson, I. R.: Effects of bed inclination and topography on steady isothermal ice sheets. *J. Glaciol.* **28**(98), 71–90 (1982)
10. Paterson, W. S. B.: *The physics of glaciers*. Pergamon, Oxford, 3rd edition (1994)
11. Schoof, C.: Basal perturbations under ice streams: form drag and surface expression. *J. Glaciol.* **48**, 407–416 (2003)
12. Siegert, M. J., Fujita, S.: Internal ice-sheet radar layer profiles and their relation to reflection mechanisms between dome c and the transantarctic mountains. *J. Glaciol.* **47**(157), 205–212 (2001)